A Method for Imaging Therapeutic Doses of Iodine-131 with a Clinical Gamma Camera

Kenneth R. Pollard, Alden N. Bice, Janet F. Eary, Lawrence D. Durack, and Thomas K. Lewellen

Department of Radiology, University of Washington Medical Center, Seattle, Washington

Imaging therapeutic doses of ^{131}I-labeled monoclonal antibody would provide valuable biodistribution data for dosimetry, but gamma cameras are unable to accurately handle the corresponding high counting rate. To image patients undergoing radioimmunotherapy, we attached 1.6- to 6.4-mm-thick Pb sheets to the front face of a high-energy parallel-hole collimator. With this method, we were able to acquire planar images of up to 700 mCi of radiolabeled antibody 1 hr after infusion. Monte Carlo simulations indicated that less than 7% of the events counted in the photopeak window were due to 364-keV photons that scattered in the Pb attenuator. Measurements indicated that the Pb sheets degraded system resolution by no more than 13%. A quantitative comparison of trace and therapy biodistribution data from planar images of the same patient was made using corrections for Pb sheet attenuation and camera deadtime.

J Nucl Med 1992; 33:771-776

Radiolabeled monoclonal antibodies continue to offer promise in the detection and treatment of cancer (1-3). Recently, Eary et al. (4) and Press et al. (5) reported success in the treatment of B-cell lymphoma using a monoclonal antibody to deliver high radiation doses to tumor tissue, up to 4300 rads from 130 to 680 mCi of ^{131}I. In this treatment protocol, a patient who fails conventional therapy for lymphoma is studied with a "trace" (5-10 mCi) dose of a radioiodinated monoclonal antibody. If the tracer biodistribution is favorable (greater absorbed dose delivered to tumor than any normal organ), then radioimmunotherapy, consisting of a single, large-dose infusion of a ^{131}I-labeled monoclonal antibody, is administered.

The treatment hypothesis of Eary et al. (4) is this: the biodistribution of a high-specific-activity therapeutic dose is similar to that observed with the lower specific-activity trace-dose study. Accordingly, biodistribution data from the trace dose study can be used to predict the radiation dose to tumor and normal organ of the therapy dose. Serum clearance data from patients after therapy suggests this is a reasonable assumption. Acquisition of organ time-

activity curves generated from images of therapeutic doses, compared to data from the trace dose study, would directly test this hypothesis. Current generation gamma cameras with standard imaging equipment, however, are not capable of accurately imaging hundred millicurie amounts of ^{131}I because of high count rate effects such as deadtime and photomultipler tube (PMT) patterns. For example, by extrapolating from the counting rates of smaller amounts of ^{131}I doses (e.g., <50 mCi) imaged on our GE 3000 XC/T gamma camera (6,7), we estimate that the full-spectrum counting rate for our largest therapeutic doses would exceed 1,000,000 cps, if the camera could acquire at that rate. However, the maximum full-spectrum counting rate of the camera is 541,000 cps. Furthermore, based on the presence of PMT patterns in uniform flood studies, image degradation becomes significant at full-spectrum counting rates above 350,000 cps. Therefore, to image radioimmunotherapy patients and verify the dosimetric predictions of the trace antibody study, incident photon flux must be reduced before it impinges upon the gamma camera detector-crystal (Fig. 1).

Two methods are obvious for substantially reducing camera event burden in this situation: (1) use of a very low-sensitivity collimator or (2) use of an attenuating medium between the patient and camera. Unfortunately, most gamma cameras are not designed to safely handle the extra weight of low-sensitivity high-energy collimators (i.e., to maintain acceptable image resolution, a low-sensitivity high-energy collimator would need very long holes, with a weight exceeding several hundred pounds). Furthermore, several of these special and expensive collimators would be needed to match the order-of-magnitude count-rate variation seen among patients receiving radioimmunotherapy with ^{131}I.

Use of a Pb (lead) attenuating sheet to reduce camera counting rates is a simple, inexpensive and flexible approach to imaging high activity sources. Reduction of count rates by absorbers has been reported before, but that work concentrated on lower-energy radionuclides and smaller amounts of radioactivity. Muehllehner et al. (8) used an Sn-Cu filter, while Pillay et al. (9) used a filter made of Pb-Zn-Sn; both for imaging ^{99m}Tc. Wiarda (10) reported the use of a Cu filter to eliminate the low-energy (30 keV) K x-rays from dose calibrator measurements of ^{123}I, ^{127}Xe, ^{133}Xe, and ^{99m}Tc. All three reported photopeak
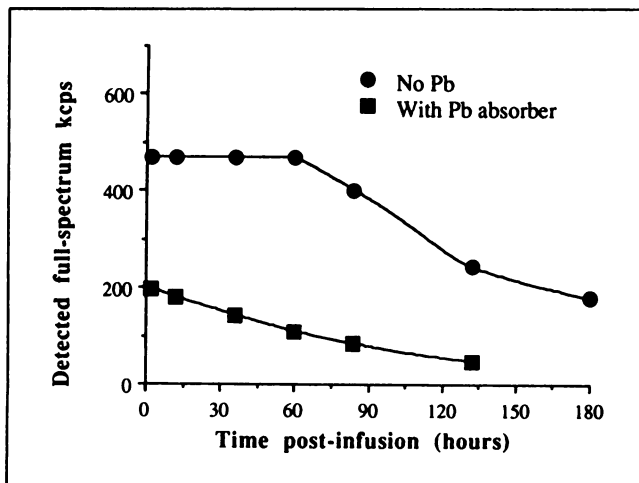
FIGURE 1. Saturation of camera counting rate. The upper curve indicates the displayed full-spectrum counting rate as a function of time after infusion. The lower curve indicates the full-spectrum counting rate for the same patient, but with the Pb sheets in place. Due to its sampling frequency, the camera's real-time display indicates saturation at 469 kcps, while the camera images indicate that saturation occurs at 541 kcps (compare to Fig. 3).

counting rate reductions of 16% or less for photopeak energies of 140 keV or greater.

To image therapeutic levels of ^{131}I with a clinical gamma camera, it is necessary to reduce the counting rate by factors of 2-10, depending on the patient's body size and on the amount of ^{131}I administered. The use of absorbers requires substantial amounts of material because of the high energy of ^{131}I gamma-rays (364 keV). This aspect raises questions about image spatial resolution and increased scatter events.

In this paper, we report our initial evaluation of placing Pb absorber sheets between patient and camera to allow imaging of therapeutic doses of ^{131}I-labeled antibody. We present results of Monte Carlo simulations, spatial resolution measurements, camera deadtime estimation and correction for ^{131}I and patient imaging data.

MATERIALS AND METHODS

Patient Studies

Planar imaging was performed on 12 radioimmunotherapy patients (8 lymphoma patients and 4 leukemia patients). Trace-labeled antibody studies involving 5-10 mCi of ^{131}I were first performed on each subject using a GE 400 AT gamma camera as previously described (4).

After infusion of the therapeutic dose, planar images of the patient's chest, abdomen and pelvis were acquired with a GE 3000 XC/T camera (6,7). Imaging began on the day of ^{131}I injection, followed by daily or twice daily imaging, depending on the effective half-life of the radiolabeled antibody. A Pb attenuator, consisting of Pb sheets up to 6.4 mm thick, was attached to the patient side of the high-energy collimator. (We used 50 cm × 50 cm × 1.6 mm (1/16 in.) Pb sheets and trimmed the corners of

the sheets to reduce the amount of unnecessary weight. By stacking four of these sheets, the 6.4 mm thick absorber was created.)

With the use of an empirical dose-to-count-rate relationship, the thickness of the Pb absorber (e.g., 1.6, 3.2, 4.8, or 6.4 mm) was chosen to prevent whole-camera count rates from exceeding 350,000 events per second. For events above this count rate, PMT patterns became noticeable in uniform flood studies. A Pb thickness was chosen before acquiring the first post-therapy-infusion image, and that thickness was used for all subsequent therapeutic images acquired over the next 3-9 days. An experimental measurement of Pb attenuation was obtained by imaging subjects with and without the Pb sheet on the final day of therapeutic imaging (and therefore at a relatively low camera counting rate).

Biodistribution data in the form of time-activity curves for tumor sites and normal organs were derived from selected image regions of interest (ROIs). Comparisons of trace and therapeutic dose time-activity curves were performed after correcting the therapy data for differences in ^{131}I sensitivity between the 400 AT and 3000 XC/T cameras, Pb absorber attenuation and camera deadtime.

Deadtime Correction Method

We used an empirically based deadtime correction to estimate the deadtime for a given imaging session. This correction was based on data collected from imaging a water-filled fishtank (17.5 × 41 × 30.5 cm³) in which increasing amounts of ^{131}I were stirred. The water in the fishtank was used as a scatter medium to produce an approximation of the energy spectrum present in a patient study. Images were acquired on the GE 3000 XC/T in 256 by 256 word mode. Starting with no activity in the fishtank, we acquired images and added increasing amounts of ^{131}I, up to a total of 52 mCi.

We assumed images acquired at low activity rates were essentially free of deadtime loss. Data from the three lowest activity levels, corresponding to 0.85, 1.65, and 3.14 mCi of ^{131}I in the fishtank, were used to estimate the true counting rate.

Simulation

A FORTRAN Monte Carlo computer code was written by Dr. Bice to examine the prevalence of Pb sheet-induced scatter in this experimental system. A three-dimensional Pb absorber sheet, a parallel-hole, high-energy Pb collimator and a 9.5-mm-thick NaI detector crystal were simulated. The simulated collimator consisted of square holes, for ease of coding and reduction of computing time, while the actual 3000 XC/T system collimator has hexagonal holes. Simulated 364-keV photons were emitted isotropically from a 1-cm square area 10 cm above and parallel to the Pb absorber sheet. No Monte Carlo biasing, weighting or stratification schemes were employed to increase computational efficiency. Multiple Compton scattering and photoelectric absorption were allowed in the Pb sheet, in the collimator, and in the NaI crystal. Photons were allowed to deposit from 0 to 364 keV in the NaI crystal. Gamma camera electronics were not simulated, but the effects of system energy resolution were included by convolving the energy spectra with a Gaussian function to approximate 10% energy resolution. Photons that interacted in the Pb absorber and ultimately deposited enough energy in the NaI crystal to fall within a 13% photopeak window (as used in our ^{131}I patient studies and representing the FWHM of the photopeak) were tabulated.

Measurement of Image Resolution Degradation

Iodine-131 impulse spread functions (ISFs) were measured with a 13% symmetric photopeak window on a GE 3000 XC/T gamma camera equipped with a high-energy collimator. We have used the ISF rather than the standard terminology, point spread function (PSF), to distinguish between the methods of experimental set-up. A relatively large level of radioactivity was needed to maintain adequate camera count rate when the thickest Pb sheet was in place. To limit our exposure to radiation during the experiment, a 30-mCi ^{131}I source of 0.5 cc volume was placed inside a collimated Pb pig positioned 10 cm above the camera. The cylindrical Pb pig had 2.5-cm thick sides and a 1.4-cm-thick base through which a 2-mm diameter hole was drilled. This modified pig collimated the 30-mCi source for measurement with the gamma camera.

With the collimated ^{131}I source in air, five images were acquired, one each with 0, 1.6, 3.2, 4.8 and 6.4 mm of Pb absorber sheets attached to the front surface of the collimator.

Camera Count Rate Performance

We previously reported on the count rate capability of the GE 3000 XC/T camera (6,7). Those tests were performed according to NEMA standards using [99m]Tc (11). For ^{131}I, we evaluated the count rate performance of the camera for its whole spectrum (0–450 keV) and for the 13% photopeak window. True versus observed count rate curves were obtained by imaging known amounts of ^{131}I activity in a 3-cc vial positioned 3.5 meters from the uncollimated camera face. Amounts of ^{131}I ranging from 0.025 mCi to 22.4 mCi and corresponding to observed whole-camera count-rates of 1.8 and 540 kcps, respectively, were used. Three low-activity measurements were averaged and used as event-loss-free points, from which the true counts at other activities were extrapolated. Several weeks later these count rate tests were repeated with the same results.

Measurement of Camera Sensitivities

We measured the relative sensitivity of the 400 AT and 3000 XC/T gamma cameras using a one-liter culture flask filled with 1 mCi of [131]I. The 3000 XC/T's NaI detector crystal was 9.5-mm thick, and the 400 AT's was 12.7-mm thick. Each camera was equipped with a high-energy, parallel-hole collimator. The 3000 XC/T collimator had septa 55 mm long and 1.9 mm thick, with holes of 4.5 mm diameter. The 400 AT collimator had septa 40 mm long and 3.2 mm thick, with holes 4.0 mm in diameter. The ratio of the 3000 XC/T counting rate to the 400 AT counting rate was measured at 0.88.

RESULTS

Simulation

Table 1 presents the Monte Carlo estimates of Pb-absorber-sheet-induced scatter. Percentage of all recorded 364-keV photons (from a simulated source in air) that Compton-scattered in the absorber sheet are tabulated for each Pb thickness. Results are for a 13% photopeak window, which was used to match that employed in patient imaging. As would be expected, thicker absorbers contributed increased scatter to the image, but even for the thickest Pb sheet, 6.4 mm, this scatter amounted to less than 7% of the detected counts.

TABLE 1
Monte Carlo Estimates of Pb-Absorber-Sheet-Induced Scatter

Pb thickness (mm)	Percent scatter*
1.6	1.8
3.2	3.7
4.8	5.5
6.4	6.7

* Percent of simulated 364-keV photons that scattered in the Pb abosrber and were detected in the 13% photopeak window.

Measurement of Image Resolution

The ISFs measured on the GE 3000 XC/T with an ^{131}I source in air are shown in Figure 2. With no Pb absorber and only the manufacturer's high-energy collimator, the FWHM value was measured at 13.9 mm. This spatial resolution degraded slightly to 15.7 mm with the thickest (6.4 mm) Pb absorber sheet in front of the collimator. These values may be compared with the manufacturer's resolution specification of 19.0 mm (FWHM), which was acquired with a 20% photopeak window (12).

GE 3000 XC/T [131]I Count Rate Performance

As indicated in Figure 3A, there is virtually no event loss from the full-energy spectrum of ^{131}I in air up to the camera saturation limit of 541 kcps. These full-energy spectrum findings are similar to what was observed with ^{99m}Tc and are consistent with the special pulse-tail-extrapolation electronics included in this camera model (6,7). In the 13% [131]I photopeak window (Fig. 3B), a 20% loss occurred at 42 kcps, corresponding to 440 kcps full-spectrum. At 541 kcps, the 13% photopeak window reported 52 kcps with a 23% deadtime loss.
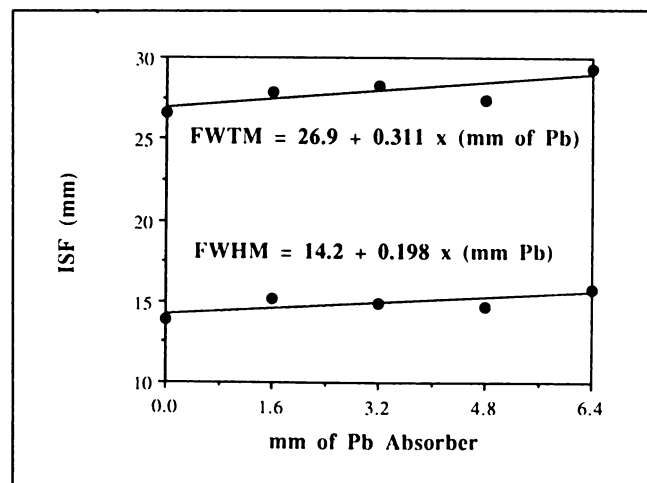

FIGURE 2. FWHM and FWTM of the ISF as a function of Pb absorber thickness. A collimated ^{131}I source was positioned 10 cm from the front face of the high-energy collimator. Results of linear regression are shown on the graph.
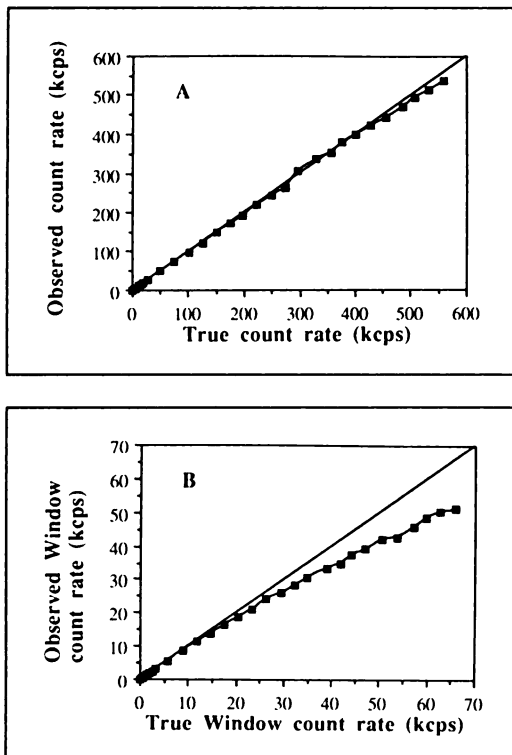
FIGURE 3. Iodine-131 count rate characteristics of the GE 3000 XC/T gamma camera. (A) The full spectrum observed versus true count rate as determined from image data. Very little data loss is indicated up to camera saturation of 541 kcps. (B) Observed versus true count rates for the 13% symmetric photopeak window which was used in patient imaging. The 13% window represents the FWHM of the detected photopeak.

Deadtime Correction

Full-spectrum counting rates were plotted, and a line representing the "true" counting rate was calculated as described in the Methods section. The deadtime correction factor as a function of the full-spectrum counting rate was found to be:

Deadtime correction factor
$$= a_0 + (a_1 \times (FSCR)) + (a_2 \times (FSCR)^2), \quad Eq.1$$

where FSCR = observed full-spectrum counting rate in cps, $a_0 = 0.990$, $a_1 = 5.45 \times 10^{-7}$ cps^{-1}, and $a_2 = 8.91 \times 10^{-13}$ cps^{-2}. Observed counts in a given ROI were multiplied by this factor to estimate the true counting rate.

Patient Studies

Figure 4 shows planar images of a lymphoma patient with a trace dose (9.9 mCi) and a therapeutic dose (443 mCi) of ^{131}I-labeled antibody. The middle column of Figure 4 is anterior planar images acquired without the Pb absorber sheet. The right column shows the same anterior patient views acquired with a 6.4-mm thick Pb sheet. These images were taken 16 hr after therapy infusion. A groin tumor, labeled by the ^{131}I-antibody, is visible, as are other structures such as the bladder and the liver. The middle

column images were acquired at a saturated camera counting rate of 541,000 cps, and PMT patterns are prominent.

The left column of images shows trace dose study images of the same patient 43 hr after radiolabeled antibody infusion. Comparison of the images in the left and right columns shows that image resolution is not significantly degraded when using the Pb absorbers. This agrees with the spatial resolution results presented above. Image format differences are due to the fact that the trace dose study was acquired on the GE 400 AT camera and the therapy study on the GE 3000 XC/T camera. There is also a difference in high-energy collimator design for each camera, with the 400 AT having thicker collimator septa, as is evident by the septal pattern in the left-hand column of images. Due to the design of its high-energy collimator, septal patterns are not present in the 3000 XC/T images at any counting rate.

Figure 5 shows time-activity curves for a 225-pixel square ROI on the liver of another patient who received trace and therapeutic antibody infusions. The therapeutic dose was 605 mCi of ^{131}I-labeled antibody. The lower curve ("trace") is from the trace dose study imaged on the 400 AT camera. The middle curve ("therapy") is from the therapeutic dose study, which was imaged on the 3000 XC/T camera; these data were corrected for camera deadtime, Pb sheet attenuation and relative camera sensitivity. The third curve ("scaled trace") is the trace dose data scaled upward by the ratio of ^{131}I activities used in the two studies, i.e., 605/9.9. Figure 5 indicates that the clearance of radiolabeled antibody from this liver is similar for both the trace and therapy studies. Furthermore, the trace dose study was predictive of the absolute ^{131}I accumulation in the liver during therapy. Trace dose and therapeutic serum clearance curves were also similar.

DISCUSSION

Previously, few methods existed for obtaining data on the biodistribution of radiolabeled antibodies in patients receiving radioimmunotherapy. Patient urine, serum clearance data and whole-body counting have been used to assess the biodistribution and dosimetry predictions of trace dose radiolabeled antibody for the behavior of the therapy dose (4). We have outlined a method that uses a standard clinical gamma camera for imaging patients infused with hundreds of mCi of ^{131}I-labeled monoclonal antibodies for therapy. This imaging technique allows the direct determination of organ and tumor biodistribution for calculation of dosimetry estimates and correlation with patient clinical response.

In order to image 100–700 mCi of ^{131}I, it was necessary to artificially reduce the gamma camera event-burden from rates in excess of 1,000,000 cps to rates under 350,000 cps. For cost and implementation reasons, we chose to use absorber sheets in front of the high-energy collimator. Image quality was only modestly degraded. An alternative method would be to use a much lower sensitiv-
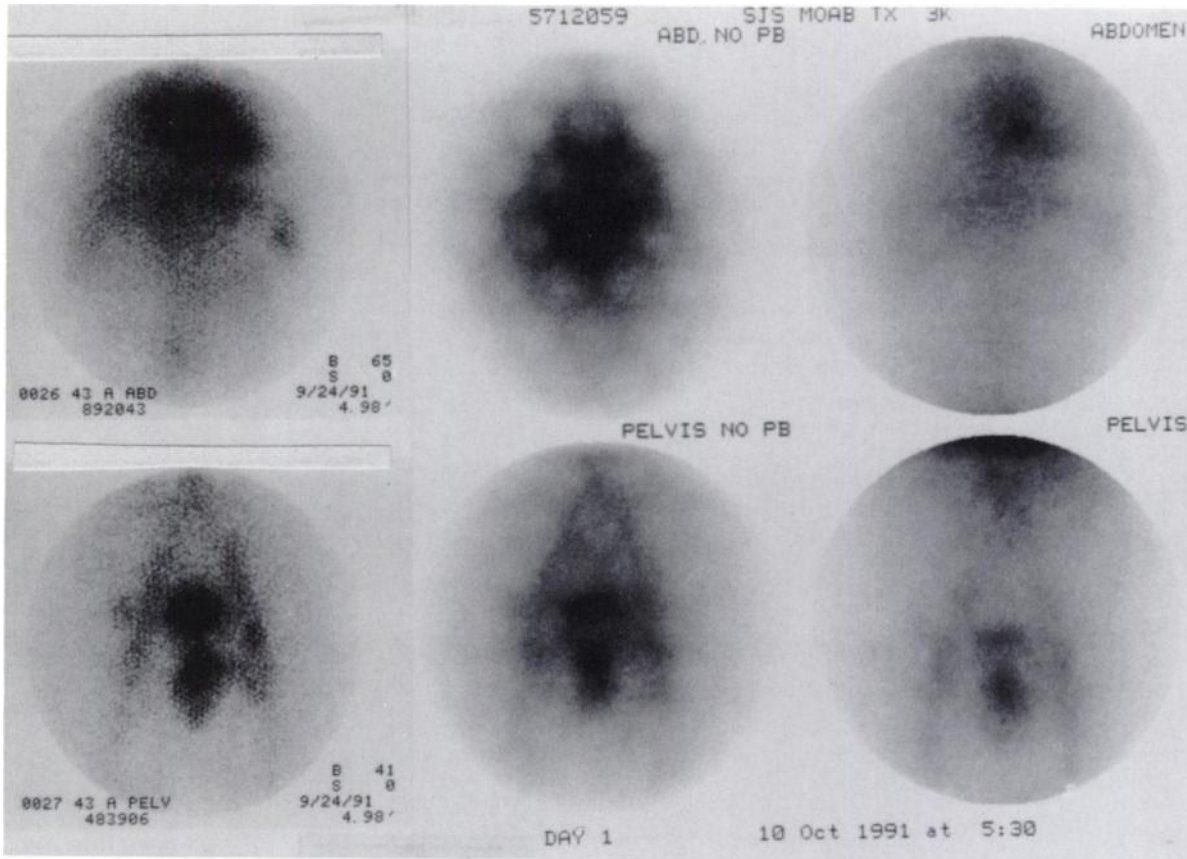
FIGURE 4. Planar images of a lymphoma patient. Top row images are of the anterior chest, and bottom row images are of the anterior abdomen. Trace dose images, acquired 43 hr after infusion of 9.9 mCi of ^{131}I, are shown in the left-hand column. Therapeutic dose images, acquired 16 hr after infusion of 605 mCi of ^{131}I, are shown in the center (without Pb sheets) and right-hand columns (with Pb sheets).

ity collimator. This approach has the advantage of reducing ^{131}I septal penetration present in all high-energy collimators, while at the same time improving planar spatial resolution. For gamma camera systems capable of han-

FIGURE 5. Time-activity curves from a 225-pixel ROI drawn on images of a human liver. Triangles indicate the cps in the ROI during the trace-labeled antibody study. Circles represent cps in the ROI during therapy. Squares represent trace cps scaled by the ratio of relative ^{131}I doses (therapy/trace).

dling the increased collimator weight, this would be an ideal approach to imaging radioimmunotherapy patients.

We chose Pb as the absorber material. Because of the high energy of ^{131}I photons (364 keV), the absorber material should have the highest atomic number possible for increased photoelectric absorption probability relative to Compton scattering. Pb, with an atomic number of 82, reasonably satisfies this criterion, although not perfectly. Lower energy photons (energy $<$ ~150 keV) are preferentially absorbed by Pb; reduction of the full-spectrum camera count rate occurs by attenuation of the primary photons and substantial reduction in numbers of patient-scattered photons.

We selected the minimum Pb sheet thickness needed to keep the observed camera rates below ~350,000 cps at any time. Although the data were not presented, we evaluated the camera image uniformity as a function of the whole camera count rate using a fillable ^{131}I flood source. For the observed rates of 350,000 cps, the PMT pattern became quite noticeable (middle column of Fig. 4). Although one of our commercially available gamma camera systems has, as a standard feature, pulse-tail extrapolation electronics to enhance count-rate capability (6,7), most current generation digital gamma cameras also have count-rate capa-
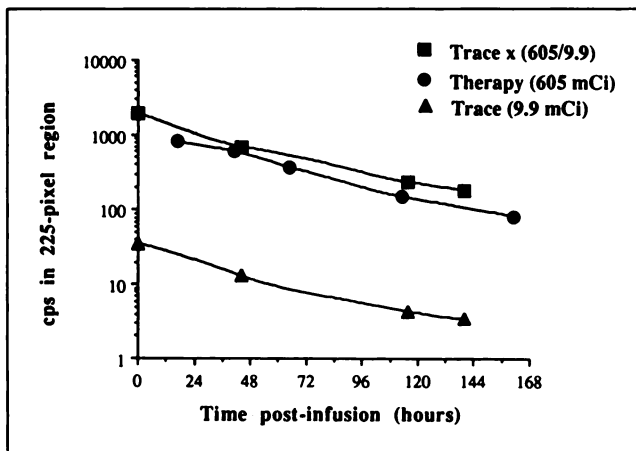
bilities suitable for imaging ^{131}I therapy patients using absorber sheets. Nonetheless, it is important that any gamma camera system proposed for use in imaging therapeutic levels of ^{131}I be carefully evaluated to determine its count-rate limitations.

The requirement of reducing camera count rates with absorber sheets has prevented us from performing SPECT imaging of therapeutic doses. Although not impossible, SPECT imaging could be cumbersome with the technique we have outlined because the camera system must be able to accurately rotate the additional weight. Other engineering problems include designing a safe method of attaching Pb sheets weighing from 30 to 50 pounds to the front face of the collimator.

There are well known limitations to planar imaging methods of estimating in vivo radiotracer concentrations (13,14). However, for relative comparison of radiotracer concentrations in multiple studies of the same subject, planar imaging can be precise (14). A comparison of the biodistribution of trace and therapeutic levels of ^{131}I-labeled monoclonal antibodies can be accomplished in this manner. The use of this therapeutic imaging technique will enable us to increase our understanding of radioimmunotherapy dosimetry and patient response to treatment.

ACKNOWLEDGMENTS

REFERENCES

1. Larson SM. Lymphoma, melanoma, colon cancer: diagnosis and treatment with radiolabeled monoclonal antibodies. *Radiology* 1987;165:297–304.
2. DeNardo SJ, DeNardo GL, O'Grady LF, et al. Treatment of B-cell malignancies with I-131 Lym-1 monoclonal antibodies. *Int J Cancer* 1988; 3(suppl):96–101.
3. Carrasquillo JA, Larson SM. Radioimmunoscintigraphy of lymphoma with monoclonal antibodies. *Cancer Treat Res* 1988;38:209–222.
4. Eary JF, Press OW, Padger CC, et al. Imaging and treatment of B-cell lymphoma. *J Nucl Med* 1990;31:1257–1268.
5. Press OW, Eary JF, Badger CC, et al. Treatment of refractory non-Hodgkin's lymphoma with radiolabeled MB-1 (anti-CD37)antibody. *J Clin Oncol* 1989;7:1027–1038.
6. Lewellen TK, Bice AN, Pollard KR, Zhu JB, Plunkett ME. Evaluation of a clinical scintillation camera with pulse-tail extrapolation electronics. *J Nucl Med* 1989;30:1554–1558.
7. Lewellen TK, Pollard KR, Bice AN, Zhu JB. A new clinical scintillation camera with pulse-tail extrapolation electronics. *IEEE Trans Nucl Sci* 1990;37:702–706.
8. Muehllehner G, Jaszczak RJ, Beck RN. The reduction of coincidence loss in radionuclide imaging cameras through the use of composite filters. *Phys Med Biol* 1974;19:504–510.
9. Pillay M, Shapiro B, Cox PH. The effect of an alloy filter on gamma camera images. *Eur J Nucl Med* 1986;12:293–295.
10. Wiarda KS. Use of a copper filter for dose-calibrator measurements of nuclides emitting K x-rays. *J Nucl Med* 1984;25:633–634.
11. Performance measurements of scintillation cameras. NEMA Standards Publication NU1-1986, 1986.
12. Product data, 3-190. Collimators for GE high-performance XC/T imaging detector. GE Medical Systems, Milwaukee, WI, 1990.
13. Bice AN, Eary JF, Nelp WB. Quantification of iodine-131 distribution by gamma camera imaging. *Eur J Nucl Med* 1991;18:142–143.
14. Eary JF, Appelbaum FL, Durack L, Brown P. Preliminary validation of the opposing view method for quantitative gamma camera imaging. *Med Phys* 1989;16:382–387.

SELF-STUDY TEST ANSWERS

urements. In this patient, a rather unexpectedly low bone mass was found that warrants consideration of an aggressive treatment plan. Other metabolic bone diseases need to be excluded in this patient.

Reference
1. Wahner HW. Bone mineral measurements. In: Freeman LM, Weissmann HS, eds. *Nuclear Medicine Annual 1986.* New York: Raven Press, 1986:195–226.
2. Wahner HW. Single- and dual-photon absorptiometry in osteoporosis and osteomalacia. *Semin Nucl Med* 1987;17:305–315.

ITEM 4: Acute Infarct of Bone
ANSWER: B
The images illustrate typical findings of acute infarction of the left femoral diaphysis in this 66-yr-old man. The scintigraphic studies were ordered to determine whether infection was the cause of bone pain and tenderness. The finding of decreased activity with both ^{99m}Tc and ^{67}Ga virtually excludes the possibility of infection. On bone scintigraphy alone, however, early acute osteomyelitis occasionally appears as a photon-deficient lesion because of interruption of the blood supply to the infected bone.

Chronic infarction and metastatic carcinoma generally are associated with enhanced ^{99m}Tc MDP uptake. The uptake of ^{67}Ga in a region of chronic infarction is variable, but will be less than that seen with ^{99m}Tc MDP. Depending on the specific carcinoma, ^{67}Ga uptake in a metastasis that was photon-deficient on bone scintigraphy would likely be increased because of gallium accumulation in the tumor tissue. Bone scintigraphy in uncomplicated leukemia (particularly chronic leukemia) is normal, but increased activity may be seen if there is cellular packing of the medullary cavity. In children with acute leukemia, focal metaphyseal lesions resembling metastases may be seen. Also, in acute leukemia, ^{67}Ga scintigraphy often shows a generalized increase in skeletal accumulation of tracer, but the appearance is more often normal with chronic leukemias.

References
1. Amundsen TR, Siegel MJ, Siegel BA. Osteomyelitis and infarction in sickle cell hemoglobinopathies: differentiation by combined technetium and gallium scintigraphy. *Radiology* 1984;153:807–812.
2. Armas RR, Goldsmith SJ. Gallium scintigraphy in bone infarction. Correlation with bone imaging. *Clin Nucl Med* 1984;9:1–3.
3. Bekerman C, Hoffer PB, Bitran JD. The role of gallium-67 in the clinical evaluation of cancer. *Semin Nucl Med* 1984;14:296–323.

ITEM 5: Reflex Sympathetic Dystrophy Syndrome
ANSWER: C
The three-phase scintigraphic study in Figure 4 demonstrates marked diffuse hyperperfusion and hyperemia of the right hand and wrist. There is moderate diffusely increased activity on the delayed image with periarticular accentuation. These findings are characteristic of the reflex sympathetic dystrophy syndrome (Sudek's atrophy). Among the listed options, cellulitis is the most difficult to exclude. The hyperperfusion and hyperemia would be typical findings with cellulitis but, in general, the delayed images will show only a mildly diffuse increase in tracer accumulation in the subjacent bone or bones. The presence of symptoms for several weeks also would be atypical for cellulitis; affected patients usually seek medical attention sooner than this.

It would be most unusual for acute rheumatoid synovitis to involve all